Biochemical Pharmacology 84 (2012) 172–181

Contents lists available at SciVerse ScienceDirect

Biochemical Pharmacology

journal homepage: www.elsevier.com/locate/biochempharm

SBF-1, a synthetic steroidal glycoside, inhibits melanoma growth and metastasis through blocking interaction between PDK1 and AKT3

Wanshuai Li [a], Ran Song [a], Xianying Fang [a], Lu Wang [a], Wei Chen [a], Pingping Tang [b], Biao Yu [b,**], Yang Sun [a,*], Qiang Xu [a,*]

[a] State Key Laboratory of Pharmaceutical Biotechnology, School of Life Sciences, Nanjing University, 22 HanKou Road, Nanjing 210093, China
[b] State Key Laboratory of Bio-organic and Natural Products Chemistry, Shanghai Institute of Organic Chemistry, Chinese Academy of Sciences, Shanghai 200032, China

ARTICLE INFO

Article history:
Received 23 February 2012
Received in revised form 5 April 2012
Accepted 6 April 2012
Available online 13 April 2012

Keywords:
SBF-1
Melanoma
PDK-1
AKT3
Metastasis

ABSTRACT

In the present study, we demonstrate that SBF-1, a synthetic steroidal glycoside, has a strong antitumor activity against melanoma cells *in vitro* and *in vivo*. SBF-1 induced cell cycle arrest with a reduced expression of various cell cycle related proteins in B16BL6 melanoma cells without causing apoptosis. SBF-1 dramatically inhibited kinase activity of 3-phosphoinositide dependent protein kinase 1 (PDK1) and thus down-regulated phosphorylation of protein kinase B (AKT). Among three known isoforms of AKT, PDK1 only interacted with AKT3 in B16BL6 melanoma cells, and SBF-1 almost completely blocked this interaction. In addition, adhesion to fibronectin and expression of integrin α4 were significantly reduced in a concentration-dependent manner. Knockdown of AKT3 resulted in the decrease in integrin α4 expression and cell adhesion. Moreover, SBF-1 inhibited the growth of melanoma xenografts and down-regulated the phosphorylation of AKT *in vivo*. In a mouse model of spontaneous metastasis, SBF-1 at very low doses of 1 and 3 μg/kg enormously inhibited melanoma metastasis into draining popliteal lymph nodes. Taken together, this study shows a small molecular compound SBF-1 with a very strong anti-melanoma activity both *in vitro* and *in vivo*. Its mechanism underlying such antitumor effect is related to the blockage of the interaction between PDK1 and AKT3.

1. Introduction

Melanoma is an increasingly important public health problem in the world. For example, the incidence of melanoma has been increasing faster than that of any other cancer in the United States [1]. The average increase rate was about 2.7% annually from 1986 to 2007 [2]. In 2010, there are 68,130 newly diagnosed cases of invasive melanoma and 46,770 cases of *in situ* melanoma [3]. Although a variety of anti-cancer strategies have been developed, chemotherapy remains the first-line treatment for most cancers, and dacarbazine has been used as the therapeutic standard without any proof of a real benefit in survival [4]. Anyhow, polychemotherapy regimens never showed a superior survival when compared with dacarbazine monochemotherapy in prospectively randomized trials [5]. Thus new therapeutic strategies are needed to decrease the incidence and mortality of melanoma.

The serine/threonine kinase AKT is a highly conserved central regulator of growth-promoting signals in multiple cell types. Dysregulation of AKT has been associated with a wide variety of cancers [6–10]. Although the AKT family members (AKT1, AKT2 and AKT3) share approximately 80% homology at the amino acid level with similar domain structure [11,12], there is emerging evidence that each family member has differential function depending on the cell type. For example, AKT1 is required for breast cancer development in MMTV-Her2/neu driven cancers, whereas ablation of AKT2 results in increased carcinogenesis [13]. AKT2 is amplified and over-expressed in a large fraction of pancreatic cancers and has recently been shown to be critical for the metastasis of colorectal cancers [14–16]. AKT3 activity is increased in over 70% of melanoma acting as an important cell survival factor in this type of cancer [17–21]. Of the three AKT isoforms, AKT3 likely plays a key role in melanoma cells because it is the predominately activated AKT isoform, and knockdown of AKT3 remarkably promotes cell apoptosis [20,21]. AKT is activated by a multistep process involving phosphatidylinositide phosphate-mediated recruitment of AKT and its upstream kinases, including PDK1, to the inner surface of the cell membrane [22]. PDK1 in the appropriate context phosphorylates AKT at threonine 308 to activate AKT [23]. Interaction between PDK1 and AKT1 or AKT2 has been reported previously [22,24]. However, up to now there is no report on the interaction between PDK1 and AKT3, and of course there is no attempt for

* Corresponding authors. Tel.: +86 25 83597620; fax: +86 25 83597620.
** Corresponding author. Tel.: +86 21 64166128; fax: +86 21 64166128.
E-mail addresses: byu@mail.sioc.ac.cn (B. Yu), molpharm@163.com (Y. Sun), molpharm@163.com (Q. Xu).

0006-2952/$ – see front matter © 2012 Elsevier Inc. All rights reserved.
http://dx.doi.org/10.1016/j.bcp.2012.04.006

interfering the interaction as a strategy of new anti-cancer therapy.

Recently, both natural and synthetic steroidal glycosides have showed anti-tumor activities in various tumor cell lines [25–29]. Saponin OSW-1, which contains a novel 16b,17a-dihydroxycholest-22-one aglycone unit with an acylated disaccharide at the 16-OH group, was discovered by Sashida, Mimaki, and coworkers in 1992 in the bulbs of *Ornithogalum saudersiae*, a perennial garden plant of the lily family widely cultivated in southern Africa [29,30]. OSW-1 has a relatively low toxicity for normal cells but inhibits the growth of a variety of malignant tumor cells [28]. Considerable effort has been directed toward the synthesis of OSW-1 and its analogues [26,29,31,32]. In 2004, Shi and coworkers reported a novel and efficient approach to the construction of the 16b,17a-dihydroxycholest-22-one structure, One of the 23-oxa-analogs of OSW-1 (SBF-1) prepared by this method is a more potent inhibitor of the growth of tumor cells than OSW-1 [29], but mechanisms for SBF-1's activities were not clear.

Here we demonstrate for the first time that PDK1 only interacts with AKT3 in B16BL6 melanoma cells, and the small molecule compound SBF-1, a unique saponin glycoside, blocks this interaction efficiently through inhibiting the kinase activity of PDK1 and thus down-regulating AKT phosphorylation. Such down-regulation is further linked to a very strong inhibition at very low doses of 1–3 μg/kg against melanoma growth and metastasis *in vivo*.

2. Materials and methods

2.1. Materials

SBF-1 is a synthetic steroidal glycoside [29], and its structure was shown in Supplementary Fig. 1A. For *in vitro* experiments, SBF-1 was dissolved in DMSO to a concentration of 20 mM (stock solution); for *in vivo* assay, SBF-1 was dissolved in DMSO to a concentration of 10 mg/ml (stock solution), and stored at −20 °C. Anti-AKT1 (#2938), anti-AKT2 (#3063), anti-AKT3 (#3788), anti-AKT (#4691), anti-p85 (#4257), anti-p110 (#4255), anti-CDK4 (#2906), anti-CDK6 (#3136), anti-cyclin D1 (#2922), anti-p15 (#4822), anti-phospho-FAK^{Tyr397} (#3283), anti-PTEN (#9552), anti-mTOR (#2972), anti-phospho-AKT^{Thr308} (#9275), anti-phospho-PTEN$^{Ser380/Thr382/383}$ (#9554), anti-phospho-PDK1^{Ser241} (#3061) and anti-phospho-mTOR^{Ser2448} (#2971) antibodies were purchased from Cell Signaling Technology (Beverly, MA). Anti-PDK1 (sc-17765), anti-integrin α4 (sc-376334), anti-GAPDH (sc-166545) antibodies, AKT1-siRNA (sc-29196), AKT2-siRNA (sc-38910), AKT3-siRNA (sc-38912), non-specific siRNA (sc-37007), goat anti-mouse IgG, goat anti-rabbit IgG, donkey anti-goat IgG HRP conjugated antibodies, mouse, rabbit and goat IgG were purchased from Santa Cruz Biotechnology (Santa Cruz, CA). Fibronectin (F2006) and laminin (L2020) were purchased from Sigma-Aldrich (St. Louis, MO). Isotype, anti-integrin α3, anti-integrin α4, anti-integrin α5, anti-integrin α8, anti-integrin αv, anti-integrin β1, anti-integrin β3, anti-integrin β6, anti-integrin β7, anti-integrin β8-PE labeled antibodies were purchased from BD Pharmingen (San Diego, CA). Alexa Fluor® 488 donkey anti-goat IgG (H + L) and Alexa Fluor® 594 goat anti-mouse IgG (H + L) were from Invitrogen (Carlsbad, CA, USA). 3-(4,5-Dimethylthiazol-2-yl)-2,5-diphenyltetrazolium bromide (MTT) and dimethyl sulfoxide (DMSO) were from Sunshine Biotechnology (Nanjing, China). All other chemicals were purchased from Sigma–Aldrich (St. Louis, MO).

2.2. Cell culture

Human melanoma cell line A375, A875, SK-MEL1, M14, MV3, murine melanoma cell line B16F1, B16F10, B16BL6, human breast cancer cell line MCF7, human liposoma cell line SW872, human hepatoma cell line HepG2, human lung cancer cell line A549, human cervical cancer cell line Hela, human prostate cancer cell line PC3 and human colorectal carcinoma cell line HCT116 were purchased from the Shanghai Institute of Cell Biology (Shanghai, China), maintained in DMEM (Dulbecco's modified Eagle's medium, GIBCO) supplemented with 10% FBS (fetal bovine serum, GIBCO), 100 U/ml penicillin, and 100 mg/ml streptomycin, and incubated at 37 °C in a humidified atmosphere containing 5% CO_2 in the air.

2.3. MTT assay

2×10^3 cells were seeded into 96-well plates, and incubated with various concentrations of SBF-1 at 37 °C for indicated time periods. Four hours before measurement, 20 μl/well MTT solutions (4 mg/ml in PBS) were added into the 96-well plates. After incubation at 37 °C for 4 h, the supernatants were discarded and 200 μl/well DMSO was added. Then the plates were measured under an FLx800 Fluorescence Microplate Reader (BioTek, Winooski, USA) at 570 nm. The optical density values of the wells without SBF-1 were considered as 100% cell growth rate.

2.4. Animals

Female C57BL/6J mice (6–8 weeks old) were obtained from the Shanghai Laboratory Animal Center (Shanghai, China). Throughout the experiments, mice were maintained as described [33]. Briefly, mice were fed with free access to pellet food and water in plastic cages at 21 ± 2 °C and kept on a 12-h light–dark cycle. Animal welfare and experimental procedures were carried out strictly in accordance with the Guide for the Care and Use of Laboratory Animals (The Ministry of Science and Technology of China, 2006) and the related ethical regulations of our university. All efforts were made to minimize animals' suffering and to reduce the number of animals used.

2.5. Construction of vectors and transient transfection in cells

PDK1 vector was generated by PCR with the following primers: sense, 5′-AAGCTTGCCACCGCCAGGACCACCAGCCAGCTGTATGACGCTGTGC-3′ and antisense, 5′-GAATTCTCACTGCACAGCAGCATCTGGATTGCTCTGGTACTGCTGCCT-3′ from muscle total RNA of a C57BL6/J mouse. Then the PCR fragments were cloned into Hind III/EcoR I sites of pcDNA 3.1(+) (Invitrogen).

Transient transfections were performed to transfer vectors into cells. Briefly, 2 μl lipofectamine 2000 (Invitrogen) and 2 μg plasmids were diluted in 50 μl opti-MEM (GIBCO) and mixed softly, then incubated at room temperature for 20 min before addition of another 800 μl opti-MEM. At last, the mixtures were spread onto cells and the cells were incubated at 37 °C for 6 h before switched to DMEM supplemented with 10% FBS. Then the cells were incubated at 37 °C for another 18 h. In the end, the cells were collected and prepared for the following experiments.

2.6. RNA interference

RNA interference was performed as the manufacture's protocols. Briefly, 2×10^5 cells were seeded in 6-well plates and allowed to grow to 50% confluence. Then cells were transfected with si-RNA and the medium was changed to DMEM supplemented with 10% FBS. The cells were allowed to grow for another 18 h before collected for the following experiments.

2.7. Western blot

Western blot assay was conducted as described before [34]. In brief, cells were collected and washed with ice-cold phosphate

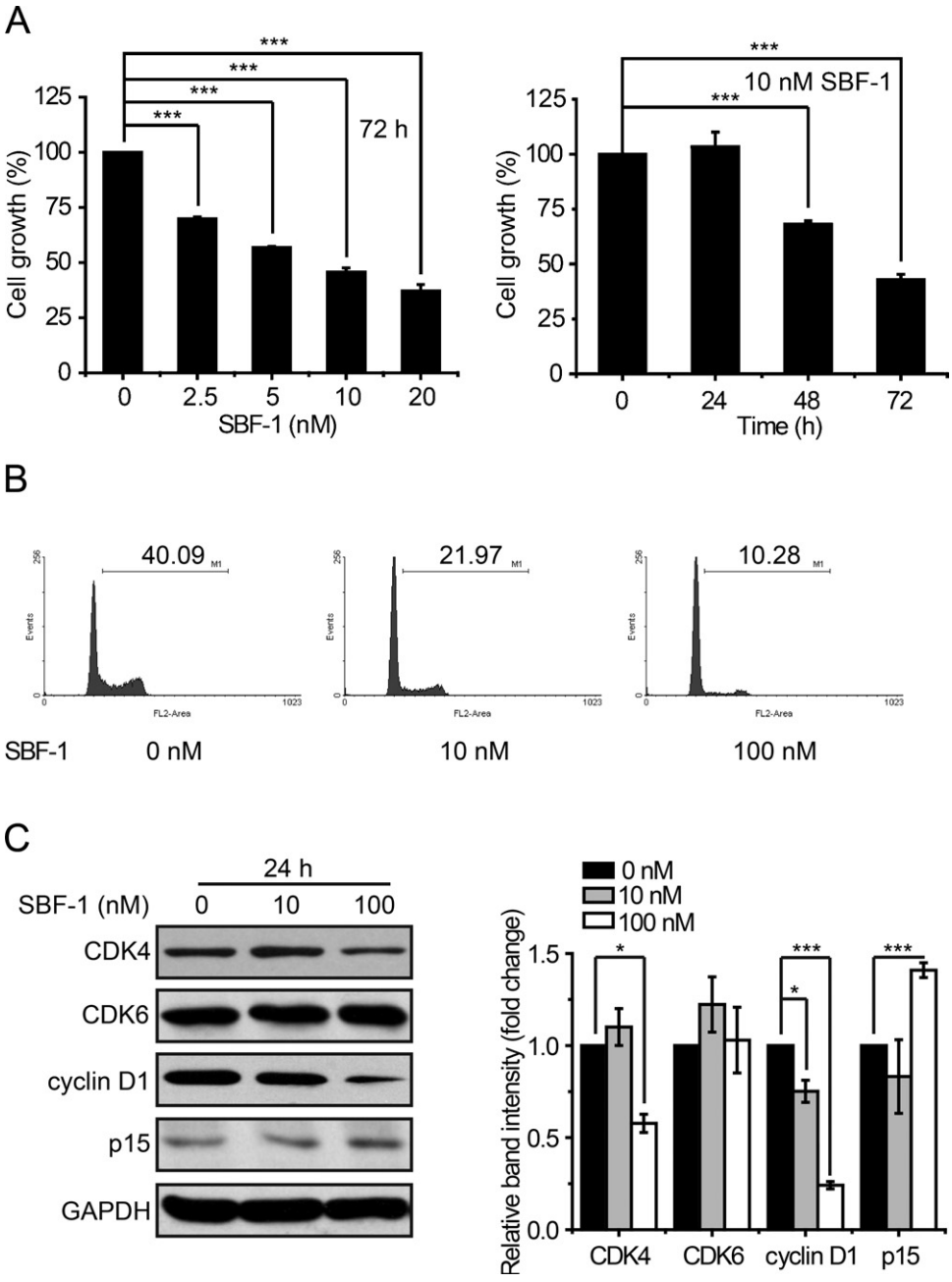

Fig. 1. SBF-1 induced cell cycle arrest in B16BL6 melanoma cells. (A) Cells were seeded in 96-well plates and incubated with or without indicated concentrations of SBF-1 for indicated time periods. Cell viability was determined by MTT assay. SBF-1 inhibited proliferation of B16BL6 cells both in a dose- (left panel) and time-dependent (right panel) manner. (B) Influence of SBF-1 on cell cycle of B16BL6 cells was determined by FCM. (C) Influences of SBF-1 on expression of cell cycle-related proteins were determined by western blotting (left panel) and relative band intensity (right panel) was analyzed by Image J software. Images were representative of more than three experiments. Error bars are means ± SD from three independent experiments. $^{*}P < 0.05$, $^{***}P < 0.001$.

buffered saline (PBS) twice before lysed in RIPA (Radio Immunoprecipitation Assay) lysis buffer (Beyotime, 50 mM Tris (pH 7.4), 150 mM NaCl, 1% Triton X-100, 1% sodium deoxycholate, 0.1% SDS, 1 mM phenylmethylsulfonylfluoride, 0.15 U/ml aprotinin and 1 mg/ml pepstatin). Then whole cell lysates were collected and for protein expression assay using respective antibodies. GAPDH was performed as a loading control.

2.8. RNA extraction and reverse transcription PCR (RT-PCR) analysis

Total RNA extraction and RT-PCR were performed as published before [35]. Briefly, cells were collected and lysed in trizol (Invitrogen). 1 μg extracted RNA was used for reverse transcription with Oligo (dT) primers (Takara). 1 μl cDNA products were used for RT-PCR analysis with primers listed in Table S1. All primers were from GenScript (Nanjing, China). cDNA amplification was performed for 30 cycles with the following settings: 94 °C for 5 min, 94 °C for 30 s, 58 °C for 30 s, 72 °C for 30 s, 72 °C for 10 min. The RT-PCR products were electrophoresed on a 2% agarose gel and visualized by ethidium bromide staining. The Gel Imaging and Documentation DigiDoc-It System (version 1.1.23; UVP, Inc., Upland, CA) was used to scan the gels. *Gapdh* was performed as a loading control.

2.9. PDK1 kinase assay

PDK1 kinase activity was determined by HTScan® PDK1 Kinase Assay Kit (Cell Signaling Technology, #7577) in accordance to the manufacture's protocols with some modifications. Briefly, 50 ng

PDK1 kinase in 50 μl reaction buffer (25 mM Tris–HCl (pH 7.5), 10 mM $MgCl_2$, 5 mM b-glycerophosphate, 0.1 mM Na_3VO_4, 2 mM DTT, 200 μM ATP, 3 μM peptide) was incubated with various concentrations of SBF-1 at room temperature for 30 min. Then add 50 μl/well stop buffer (50 mM EDTA, pH 8.0) to stop the reaction. Transfer 25 μl of each reaction to a 96-well streptavidin-coated plate containing 75 μl ddH_2O/well and incubate at room temperature for 60 min. After washing three times with 200 μl/well PBS/T (0.05% Tween 20 in PBS), dilute primary antibody (phospho-PKA/C^{Thr197} Antibody #4781) in PBS/T with 1% BSA. Add 100 μl/well diluted primary antibody and incubated at room temperature for 120 min. After washing three times with PBS/T, kinase activity was determined according to Colorimetric ELISA detection methods provided by the manufacture. In the end of the detection, the absorbance at 450 nm was read with an FLx800 Fluorescence Microplate Reader (BioTek, Winooski, USA). Relative PDK1 kinase activity was shown by $OD_{450\ nm}$.

2.10. Cell adhesion assay

Cell adhesion assay was performed using methods published before [36] with some modifications. In brief, 96-well flat-bottom plates were coated with 50 μl fibronectin (10 μg/ml) in PBS overnight at 4 °C and then blocked with 0.2% bovine serum albumin (BSA) for 2 h at room temperature followed by washing three times. Cells were added into each well in triplicate and incubated for 30 min at 37 °C. Plates were then washed three times with PBS to remove unbound cells. Numbers of cells remained bound to the plates were analyzed by MTT assay. After subtraction of the background cell binding to BSA-coated wells, the percentage of adherent cells was calculated by dividing the optical density of the adherent cells by that of the initial input cells.

2.11. Immunofluorescence

B16BL6 melanoma cells incubated with indicated concentrations of SBF-1 for 6 h were fixed in 4% paraformaldehyde (pH 7.4) for 30 min. Then cells were softly washed twice with PBS, and incubated with 0.5% Triton X-100 for 30 min. Thereafter, cells were softly washed twice with PBS and blocked with 3% bovine serum albumin for 1 h. Cells were incubated with primary antibodies (PDK1- and AKT3-specific antibody) at 4 °C overnight. After washed twice, cells were incubated with secondary antibodies for 1 h and stained with 4,6-diamidino-2-phenylindole (DAPI) for 1 min. The fluorescent signals were detected with FluoView™ FV1000 confocal microscope (Olympus Corporation, Shinjuku, Tokyo, Japan) and analyzed by Olypus Fluview Ver1.7b viewer (Olympus Corporation, Shinjuku, Tokyo, Japan).

2.12. Flow cytometry (FCM)

Flow cytometry was demonstrated as described [37]. B16BL6 melanoma cells treated with different concentrations of SBF-1 or AKT3-siRNA for indicated time periods were incubated with respective antibodies for 30 min. Isotype matched mouse IgG served as negative control. Cells were then washed twice with ice-cold PBS. Integrin expression was analyzed by a FACSCalibur Flow Cytometry and CellQuest software (BD Biosciences).

2.13. In vivo tumor growth, life span and spontaneous metastasis assay

2×10^5 B16BL6 cells were injected subcutaneously into the right parts of 6–8-week-old female C57BL6/J mice. Three days after injection, all mice formed tumors and they were distributed into five groups ($n = 12$) according to tumor volumes, and the day was marked as day 0. Vehicle (0.05% DMSO in PBS), 1 μg/kg, 5 μg/kg, 10 μg/kg SBF-1 and 1 mg/kg cisplatin were intraperitoneally injected to every group respectively every day since day 0. At the same time, body weight and tumor volumes were measured. For tumor growth assay, mice were euthanized fourteen days after inoculation, and the weight of tumor, liver and spleen were measured. For life span assay, mice were maintained until all died. For spontaneous metastasis assay, 1×10^6 B16BL6 cells were injected into the right foot-pads of 6–8-week-old female C57BL6/J mice. Ten days after injection, all mice formed tumors and they were distributed into three groups ($n = 6$) according to tumor volumes, and the day was marked as day 0. Vehicle (0.02% DMSO in PBS), 1 μg/kg and 3 μg/kg SBF-1 were intraperitoneally injected to every group respectively every day since day 0. Body weight and tumor volumes were measured at the same time. On day 12, the mice were euthanized and the draining popliteal lymph nodes of right foot-pads were taken.

2.14. Statistical analysis

Data are expressed as means ± SD. The Student's t test was used to evaluate the difference between 2 groups. Kaplan–Meier method was used to evaluate the survival test. $P < 0.05$ was considered to be significant.

3. Results

3.1. SBF-1 strongly inhibited the proliferation of B16BL6 melanoma cells

Various tumor cell lines were incubated with different concentrations (0, 1, 10, 100, 1000, 10,000 nM) of SBF-1 for 72 h, the IC50 values, defined as the concentrations that cause a 50% loss of cell viability, were determined by MTT assay and shown in Table 1. SBF-1 showed stronger inhibitory effects against these tumor cells including melanoma, breast cancer, liposarcoma, hepatoma, cervical cancer, lung carcinoma, prostate cancer, and colorectal carcinoma with an IC50 less than 600 nM. As listed in Table 1, SBF-1 showed a strongest anti-growth effect on the murine melanoma cell line B16BL6 with an IC50 of 6.9 ± 0.7 nM. So we chose B16BL6 melanoma cells for further study.

3.2. SBF-1 caused cell cycle arrest in B16BL6 melanoma cells without influencing apoptosis

2×10^3 B16BL6 melanoma cells were seeded into the wells of 96-well plates, and incubated with various concentrations of SBF-1

Table 1
IC50 values of SBF-1 in various tumor cell lines *in vitro*.[a]

Cell type	Tumor type	IC50 (nM)
A375	Melanoma	378.7 ± 34.0
A875	Melanoma	43.8 ± 3.6
SK-MEL1	Melanoma	62.6 ± 6.8
M14	Melanoma	109.3 ± 10.5
MV3	Melanoma	373.1 ± 21.2
B16F1	Melanoma	60.5 ± 4.9
B16BL6	Melanoma	6.9 ± 0.7
B16F10	Melanoma	20.8 ± 1.3
MCF7	Breast cancer	243.3 ± 18.1
SW872	Liposarcoma	357.2 ± 24.7
HepG2	Hepatoma	>1000
A549	Lung cancer	282.7 ± 21.3
Hela	Cervical cancer	302.4 ± 29.5
PC3	Prostate cancer	237.1 ± 19.3

[a] Cells were treated with various concentrations of SBF-1 for 72 h. The IC50 values shown were means ± SD from three independent experiments.

at 37 °C for 0, 24, 48 and 72 h, respectively. We observed that SBF-1 inhibited the growth of B16BL6 melanoma cells both in a concentration- (0, 10, 100, 1,000 nM SBF-1 for 72 h, Fig. 1A, left panel) and time- (10 nM SBF-1 for 0, 24, 48 and 72 h, Fig. 1A, right panel) dependent manner, respectively.

As an analog of OSW-1 [28], we supposed that SBF-1 might induce abundant apoptosis in B16BL6 cells. We next analyzed the effects of SBF-1 on apoptosis and cell cycle. B16BL6 melanoma cells (2×10^5) were seeded into 6-well plates and incubated with different concentrations (0, 10, 100, 1000 nM for apoptosis analysis and 0, 10, 100 nM for cell cycle analysis respectively) of SBF-1 for 24 h. To our surprise, SBF-1 did not influence apoptosis at all (Supplementary Fig. S2), but caused evident cell cycle arrest in G1 phase (Fig. 1B). To further confirm SBF-1's effect on cell cycle, we detected the expressions of various cell cycle related proteins, and found that the expressions of CDK4 and cyclin D1 were significantly down-regulated by 100 nM SBF-1 (Fig. 1C).

3.3. SBF-1 down-regulated phosphorylation of AKT in a concentration- and time-dependent manner

As we know, AKT is crucial for proliferation and growth of tumor cells [12,38], and inhibition of AKT activity leads to aberration of cell growth [39,40]. In the following study, we found that the phosphorylation of AKT at threonine 308 site was significantly down-regulated both in a concentration- and time-dependent manner (Fig. 2). Although SBF-1 also concentration- and time-dependently down-regulated the phosphorylation of AKT at serine 473 site (Supplementary Fig. S3), the inhibitory effect was much weaker. These results suggest that the effect of SBF-1 might rely on negatively regulating phosphorylation of AKT (mainly at threonine 308 site), which down-regulates cell cycle related proteins and causes cell cycle arrest.

3.4. SBF-1 blocked the interaction between PDK1 and AKT3

Phosphorylation of AKT can be stimulated by series of signals [11,12,22,23]. We analyzed expression changes of p85 (a regulatory subunit of phosphatidylinositol 3-kinase), p110α (a catalytic subunit of phosphatidylinositol 3-kinase), PTEN (phosphatase and tensin homolog), phospho-PTEN$^{Ser380/Thr382/383}$, mTOR (mammalian target of rapamycin), phospho-mTOR^{Ser2448}, PDK1 and phospho-PDK1^{Ser241} in B16BL6 melanoma cells after incubation with increasing concentrations (0, 10, 100, 1000 nM) of SBF-1 for 24 h. However, we did not detect any expression changes of these proteins (Supplementary Fig. S4). In the following study, we found that SBF-1 inhibited kinase activity of PDK1 (Fig. 3A), a kinase phosphorylates and activates AKT [41], in a concentration-dependent manner. To further confirm this result, we established a murine PDK1 vector and transfected it into B16BL6 melanoma cells. After transfection for 24 h, the cells were incubated with increasing concentrations (0, 100, 1000 nM) of SBF-1 for another 24 h. Compared with the cells transfected with mock vector, phosphorylation of AKT at threonine 308 site was obviously increased, and the inhibitory effect of SBF-1 on phosphorylation of AKT at threonine 308 site in the cells transfected with PDK1 vector was almost lost (Fig. 3B). Meanwhile, cell cycle arrest induced by 10 nM SBF-1 was almost abolished in cells transfected with PDK1 (Supplementary Fig. S5). Next, we measured the interaction of PDK1 with AKT isoforms in B16BL6 melanoma cells. Surprisingly, only interaction between PDK1 and AKT3 was detected (Fig. 3C). Moreover, after incubation with 1000 nM SBF-1 for 24 h, interaction between PDK1 and AKT3 could

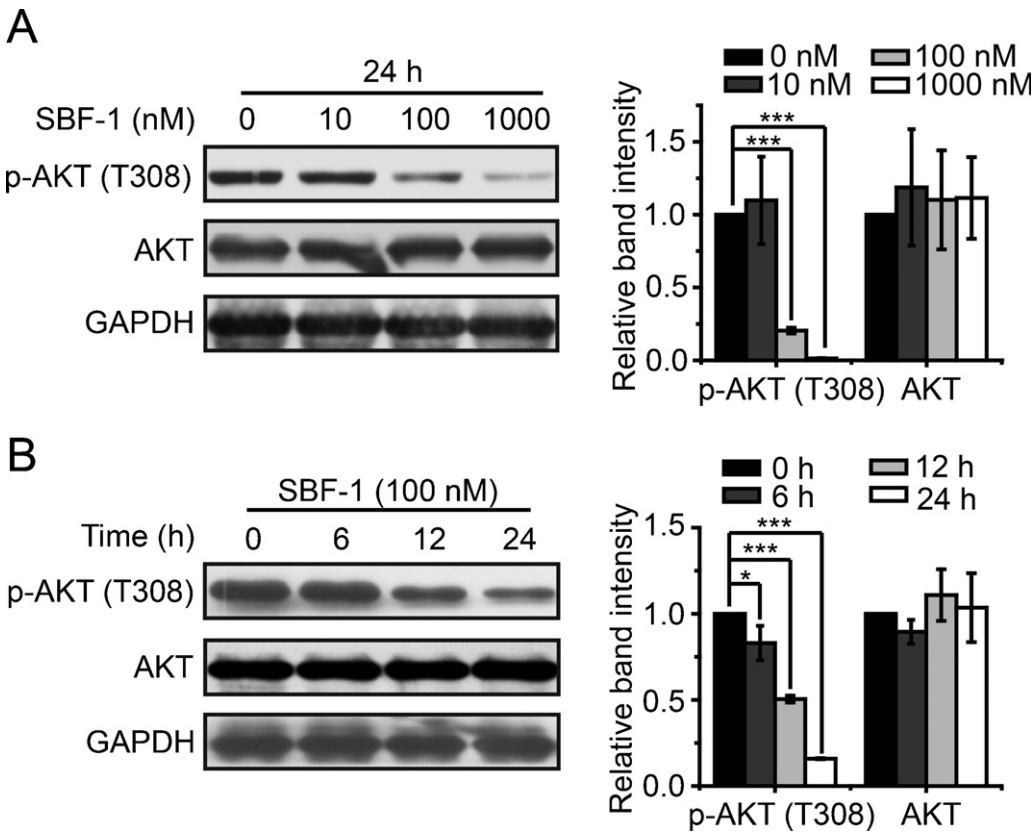

Fig. 2. SBF-1 negatively regulated phosphorylation of AKT. B16BL6 melanoma cells were incubated with various concentrations of SBF-1 for 24 h (A) or with 100 nM SBF-1 for 0, 6, 12, and 24 h (B), respectively. Expression of total AKT and phosphorylated AKT were determined by western blotting (left panel), and relative band intensity was determined by Image J software (right panel). GAPDH was performed as a loading control. Images were representative of three independent experiments. Error bars are means ± SD from three independent experiments. $^{*}P < 0.05$, $^{***}P < 0.001$.

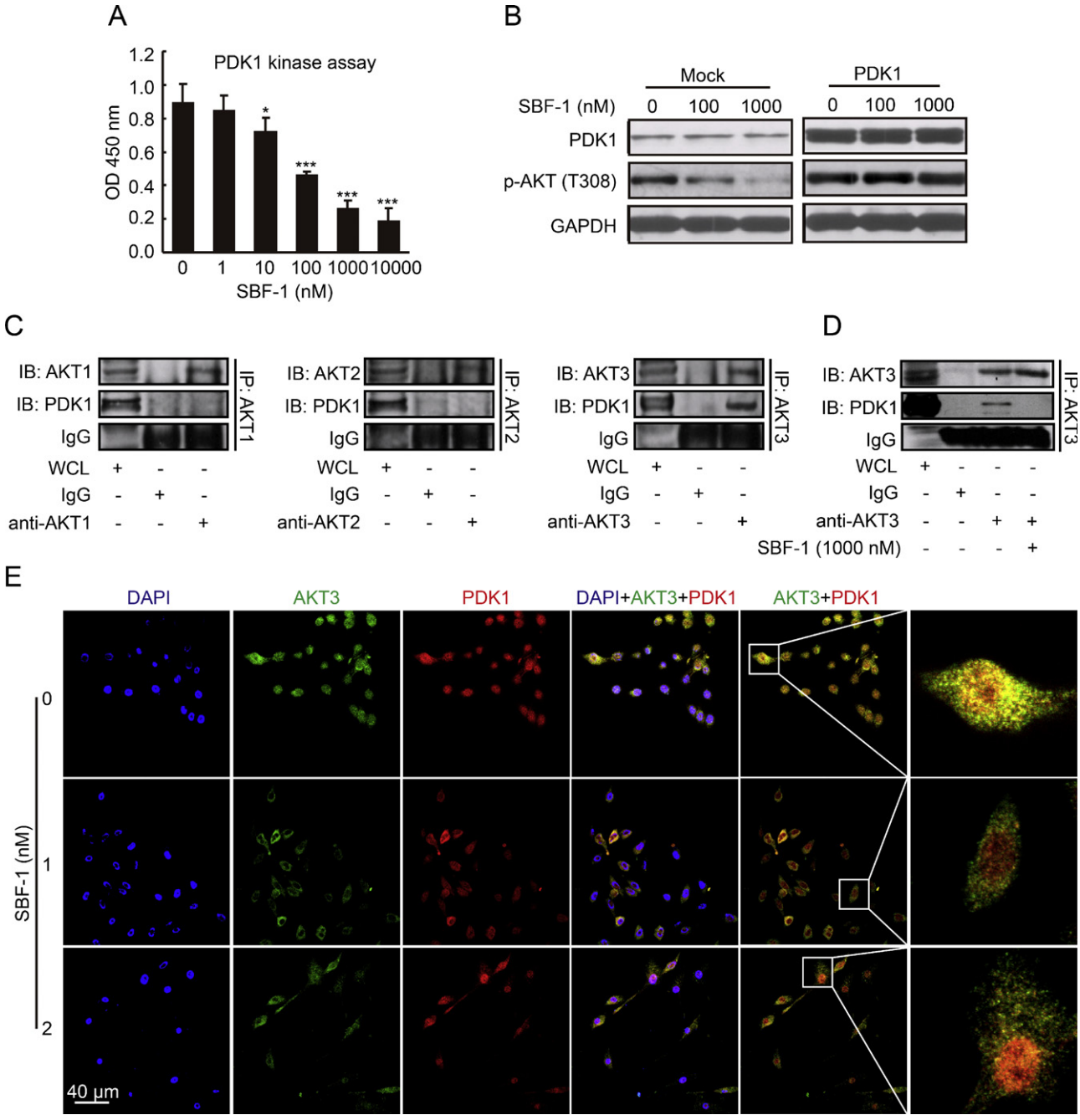

Fig. 3. SBF-1 blocked the interaction between PDK1 and AKT3 in B16BL6 melanoma cells. (A) Influence of SBF-1 on kinase activity of PDK1 was analyzed as described in materials and methods. Error bars are means ± SD from three independent experiments. $^{*}P < 0.05$, $^{***}P < 0.001$ *vs.* cells treated without SBF-1. (B) Cells were transfected with pcDNA3.1(+) (Mock) or pcDNA3.1(+)–mPDK1 (PDK1) for 24 h, then cells were incubated with various concentrations of SBF-1 for another 24 h. Protein expression was detected by western blotting. (C) WCL of B16BL6 cells were immunoprecipitated by AKT1, AKT2 and AKT3-specific antibody, respectively. Then PDK1 were detected by western blotting. IgG was performed as a negative control. (D) B16BL6 melanoma cells were incubated with or without 1000 nM SBF-1 for 24 h. Then WCL were immunoprecipitated by AKT3-specific antibody and PDK1 expression was determined by western blotting. Images are representative of three independent experiments. (E) Cells were treated with 0 nM, 1 nM and 2 nM SBF-1 for 72 h. Distribution of AKT3 and PDK1 were shown by green and red fluorescence, respectively. Nucleus were stained by DAPI and shown by blue fluorescence. (For interpretation of the references to color in this figure legend, the reader is referred to the web version of the article.)

not be detectable (Fig. 3D). In addition, co-localization of AKT3 and PDK1 was reduced obviously after exposure to 1 nM and 2 nM SBF-1 for 72 h (Fig. 3E). To firmly ensure the important of AKT3 to the phosphorylation of AKT at threonine 308 site, we knocked down AKT1, AKT2 and AKT3 with RNA interference (Supplementary Fig. S6A). Compared with si-AKT1- and si-AKT2-treated cells, phosphorylation of AKT at threonine 308 site in si-AKT3-treated cells was reduced much more obviously (Supplementary Fig. S6B). In all, these results imply that SBF-1 blocks interaction between PDK1 and AKT3, which may explain its inhibitory effect on kinase activity of PDK1.

3.5. SBF-1 inhibited adhesive ability of B16BL6 melanoma cells through down-regulating integrin α4

It is well known that adhesion plays a crucial role in metastasis of malignant tumors including melanoma. From above results, we know that SBF-1 efficiently suppressed the growth of B16BL6 melanoma cells in extremely low concentrations, we supposed that SBF-1 could also inhibit adhesion of B16BL6 cells. 2×10^5 B16BL6 melanoma cells were seeded into the wells of 6-well plates, and incubated with different concentrations (0, 1, 2, 5,

10 nM) of SBF-1 for 72 h. Then cells were collected and adhesive ability to fibronectin and laminin were detected. SBF-1 showed a significant inhibition on adhesive ability of the cells to fibronectin (Fig. 4A, left panel), while only showed slight inhibitory effects to laminin (Fig. 4A, right panel). Then we analyzed the expression of fibronectin-specific integrins (Supplementary Fig. S7A and B) and measured effects of SBF-1 on expression of integrin α4, α5 and β1, which were expressed abundantly in B16BL6 melanoma cells. Only integrin α4 was down-expressed by SBF-1 (Supplementary Fig. S7C and D). Moreover, adhesive ability of cells pre-treated with integrin α4-specific antibody was markedly reduced (Fig. 4B), and integrin α4 was down-expressed in B16BL6 melanoma cells treated with AKT3-siRNA (Fig. 4C). At the same time, AKT3-siRNA significantly reduced the adhesive ability of cells (Fig. 4D). As expected, SBF-1 inhibited the phosphorylation of focal adhesion kinase at tyrosine 397 site (FAK^{Tyr397}) (Supplementary Fig. S7E). These results suggest that SBF-1 suppresses integrin α4 and phosphorylation of FAK thus inhibits adhesive ability of B16BL6 melanoma cells, which may be due to the inhibition of AKT3 by SBF-1.

3.6. SBF-1 inhibited tumor growth and spontaneous metastasis, and prolonged life span in mice

To investigate effects of SBF-1 *in vivo*, we subcutaneously injected 2×10^5 B16BL6 melanoma cells into the right parts of C57BL6/J mice. Three days after inoculation, when all mice formed tumors, we distributed the mice into five groups ($n = 12$) and the day was marked as day 0. Vehicle (DMSO in PBS), indicated doses of SBF-1 and cisplatin (positive control) were administrated subcutaneously to the mice every day since day 0. At the same time, we measured tumor volumes and body weights until day 14. SBF-1 at the very low doses of 1, 5 and 10 μg/kg significantly inhibited the growth and weights of tumor xenografts and 10 μg/kg of SBF-1 showed a same intensity of inhibition as 1 mg/kg of cisplatin (Fig. 5A and B). It should be noted that at above doses cisplatin significantly decreased the body weights of mice while SBF-1 did not (Supplementary Fig. S8A). Also, cisplatin induced dramatic weight loss of spleen (Supplementary Fig. S8B) and liver (Supplementary Fig. S8C). We then detected phosphorylation of AKT in tumor xenografts. SBF-1 showed stronger inhibition of AKT phosphorylation than cisplatin (Fig. 5C). In life span assay, mice were allowed to live until their spontaneous death and SBF-1 had a better prolonged effect than cisplatin did (Fig. 5D).

In the spontaneous metastasis assay, 1×10^6 B16BL6 melanoma cells were injected into the right foot-pads of C57BL6/J mice. Similarly, SBF-1 had little effect on body weight (Fig. 6A), but remarkably inhibited tumor growth in a very low dose (3 μg/kg) (Fig. 6B). The control group showed 100% visible metastasis, while lower ratios of metastasis were found in SBF-1-treated groups with approximately 66.7% in 1 μg/kg group and 16.7% in 3 μg/kg group, respectively (Fig. 6C).

4. Discussion

In the initial study, we screened various tumor cell lines, and observed that SBF-1 was extremely cytotoxic to the malignant melanoma cell line B16BL6 (IC50 value was 6.9 ± 0.7 nM). This

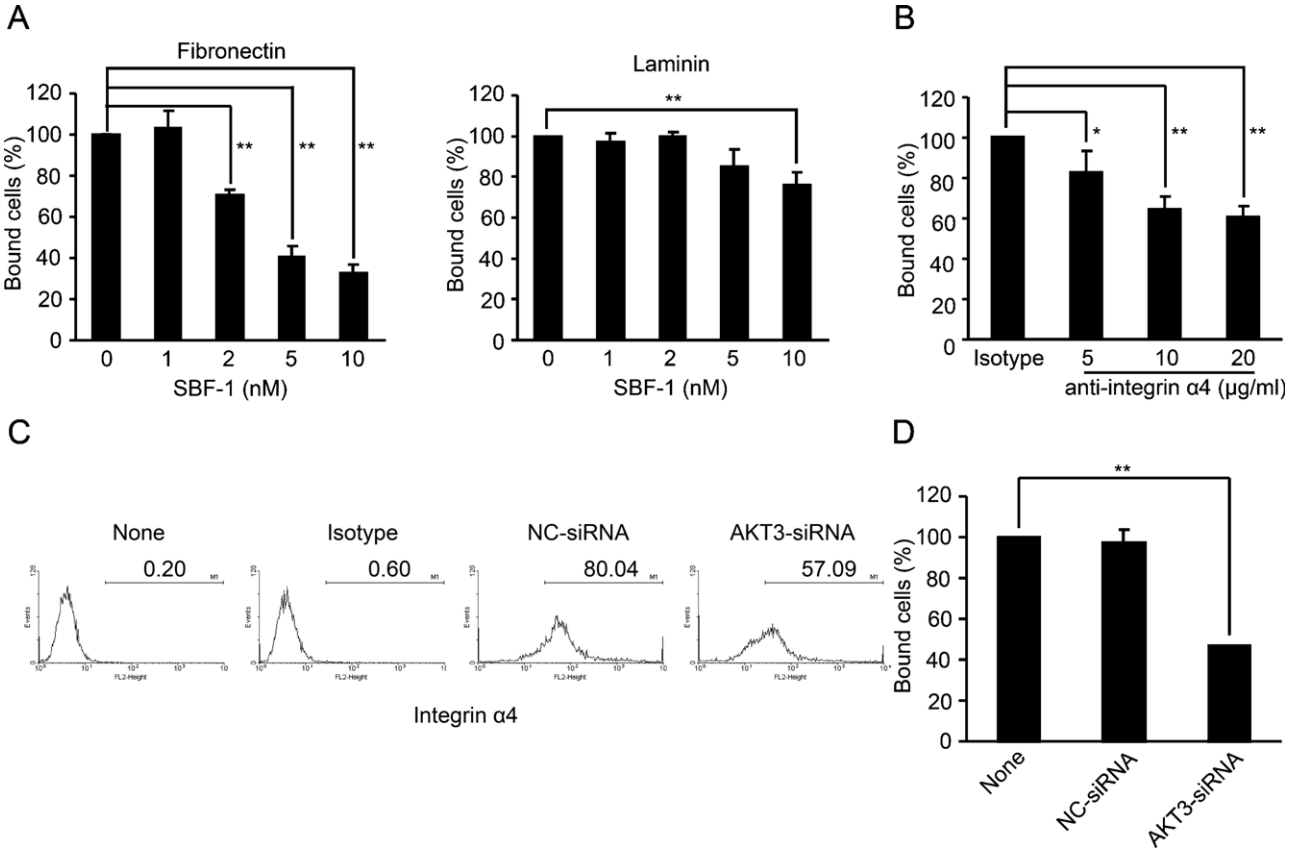

Fig. 4. SBF-1 inhibited adhesive ability of B16BL6 melanoma cells on fibronectin through negatively regulating AKT3/integrin α4. (A) Cells incubated with indicated concentrations of SBF-1 for 24 h, and cell adhesion assay was performed as described in materials and methods. Influences of SBF-1 on adhesion to fibronectin (left panel) and laminin (right panel) were shown. (B) Cells were treated with isotype IgG or anti-integrin α4 antibody for 24 h. Then adhesion to fibronectin was performed. C, Cells were transfected with non-specific siRNA (NC-siRNA) or AKT3-siRNA for 24 h. Then expression of integrin α4 was determined by FCM. (D) Adhesion to fibronectin after cells were treated with NC-siRNA or AKT3-siRNA for 24 h. Error bars are means ± SD from three independent experiments. $^*P < 0.05$, $^{**}P < 0.01$.

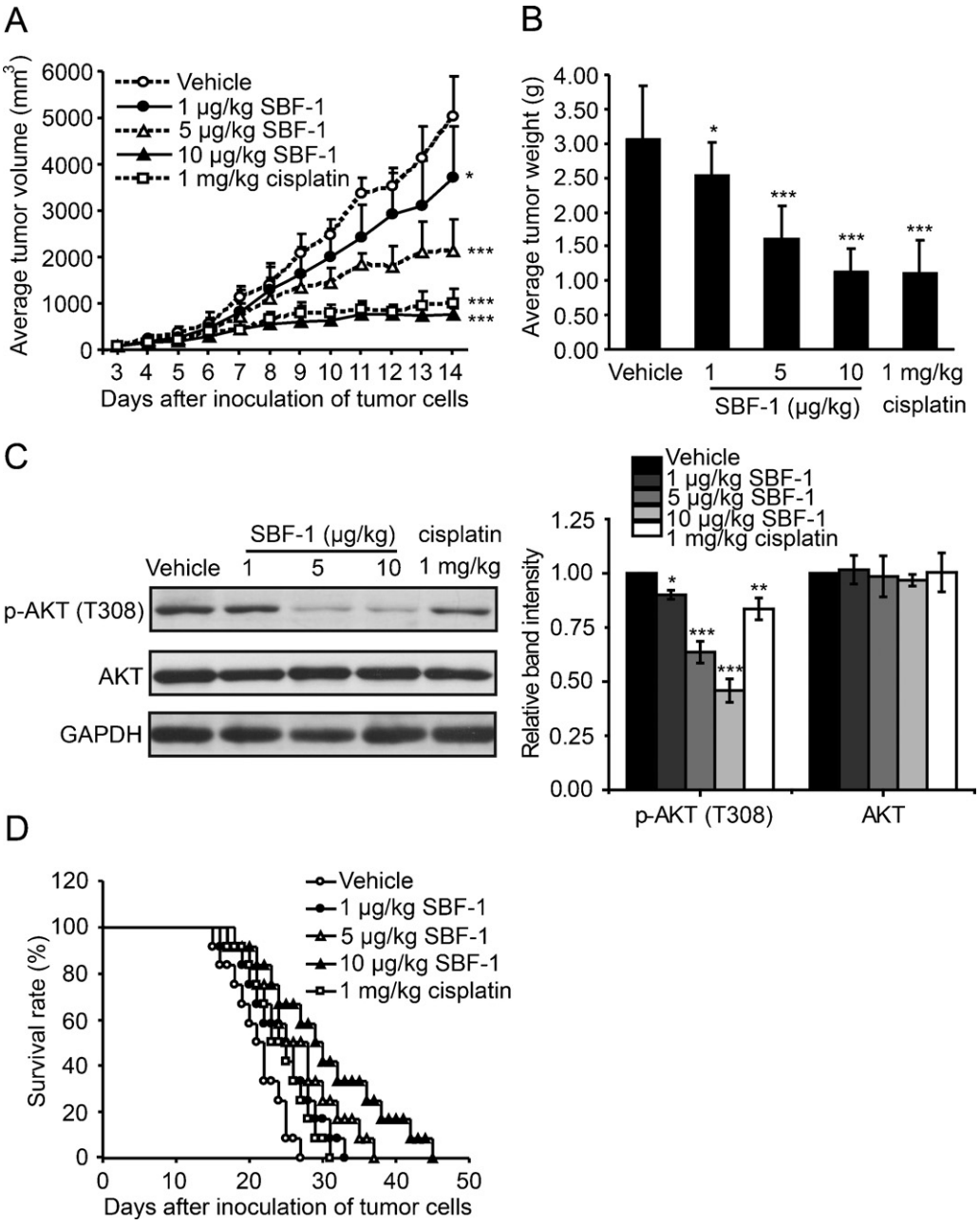

Fig. 5. SBF-1 inhibited growth of melanoma xenografts by inhibiting AKT phosphorylation. B16BL6 melanoma cells (100 μl/mouse, 2×10^6 cells/ml) were injected subcutaneously into the right flanks of female C57BL6/J mice. Indicated doses of SBF-1 and cisplatin were administrated to the mice by intraperitoneal injection every day. DMSO in PBS was injected as a vehicle control. (A) Tumor volumes. (B) Tumor weight. (C) The expression of phosphorylated AKT in tumor xenografts was determined by western blotting (left panel) and relative band intensity was analyzed by Image J software (right panel). (D) Survival curves of another experiment of melanoma xenografts ($n = 12$). Error bars are means ± SD of twelve mice in every group. $^*P < 0.05$, $^{**}P < 0.01$, $^{***}P < 0.001$ *vs.* vehicle.

phenomenon was inspiring, since the cell line was especially malignant, with great potential of growth and metastasis [42,43]. In the following study, we surprisingly observed that SBF-1 caused cell cycle arrest in B16BL6 melanoma cells, with significant down-expression of cell cycle-related proteins CDK4 and cyclin D1 and up-expression of p15, while had no effect on apoptosis.

AKT is a threonine/serine protein kinase, and has been reported to be a key regulator in survival and growth of tumors [8,9,12,38,41,44,45]. Although abundant reports mentioned the anti-tumor activities of steroidal glycosides [46,47], little reports connected AKT signaling with their activities. In our current study, we found that SBF-1 significantly inhibited phosphorylation of AKT, both in a concentration- and time-dependent manner. Moreover, when incubated with low concentrations (0, 1, 2, 5, 10 nM) of SBF-1 for a long time period (72 h), phosphorylation of AKT at threonine 308 was significantly ($P < 0.05$) inhibited by 5 nM and 10 nM SBF-1 (Supplementary Fig. S9). To investigate how SBF-1 inhibited phosphorylation of AKT, we screened various related proteins, but did not observe any expression changes. We supposed that SBF-1 would just affect kinase activity, not the expression. Interestingly, kinase activity of PDK1 was significantly inhibited in a concentration-dependent manner. Overexpression of PDK1 almost abolished inhibitory effect of SBF-1 on phosphorylation of AKT. These findings suggest that SBF-1 may directly target PDK1, and thus inhibits phosphorylation of AKT.

AKT1, AKT2 and AKT3 are three isoforms of AKT. Of three AKT isoforms, AKT3 likely plays a key role because it is the predominately activated AKT isoform in melanoma cells, and

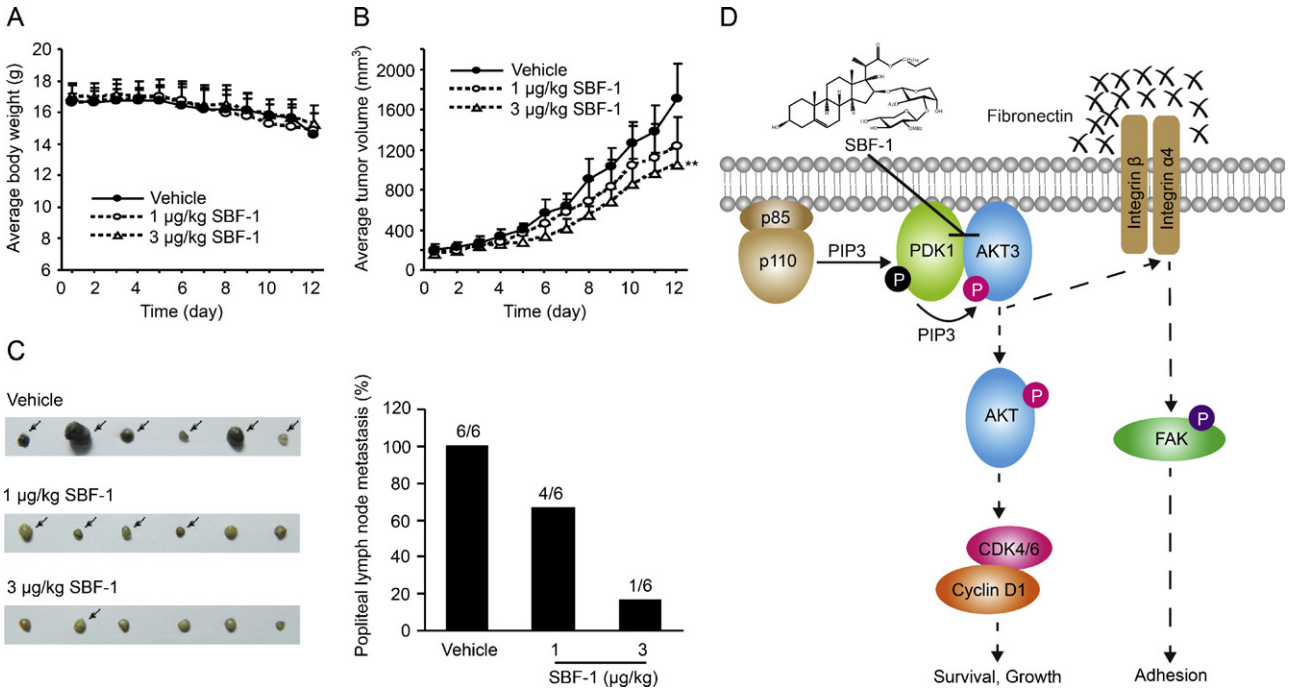

Fig. 6. SBF-1 inhibited spontaneous metastasis of B16BL6 cells in mice. 1×10^6 cells (in 20 μl PBS) were injected subcutaneously into right foot-pads of C57BL6/J mice. DMSO in PBS (vehicle control) or different concentrations of SBF-1 were administrated every day. (A) Body weight. (B) Tumor volumes. (C) On day 12, the mice were euthanized and draining popliteal lymph nodes of right foot-pads (left panel) and the ratios of visible popliteal lymph node metastasis (right panel) were shown. (D) Mechanism for SBF-1's effects on B16BL6 melanoma cells. SBF-1 blocks interaction between PDK1 and AKT3, thus inhibits phosphorylation of AKT, which induces down-expression of CDK4 and cyclin D1 and cell cycle arrest at G1 phase, and results in growth inhibition. Moreover, SBF-1 inhibits adhesion by negatively regulating AKT3/Integrin α4/FAK signaling.

knockdown of AKT3 inhibits cell growth [20,21]. Interestingly, we only observed interaction between PDK1 and AKT3 in B16BL6 melanoma cells, which had not been reported before. Moreover, after exposure to 1,000 nM SBF-1 for 24 h or 1 nM and 2 nM SBF-1 for 72 h, this interaction could not be detectable. Moreover, when AKT3 was knocked down in B16BL6 cells, phosphorylation of AKT at threonine 308 site was reduced dramatically. Thus, these results hint that SBF-1 blocks interaction between AKT3 and PDK1, which contributes to SBF-1's inhibitory effect on phosphorylation of AKT.

Metastasis is a crucial feature of malignant melanoma [48,49], and adhesive ability is a critical *in vitro* feature of metastasis [50,51]. In the following study, we observed that SBF-1 significantly inhibited adhesion of B16BL6 melanoma cells to fibronectin, while had slight effect on adhesion to laminin. As expected, integrin α4, a fibronectin-specific integrin, and phosphorylation of FAK were dramatically down-regulated by SBF-1, while had no effects on other fibronectin-specific integrins. In addition, adhesive ability of B16Bl6 melanoma cells treated with integrin α4-specific antibody was significantly inhibited. When AKT3 was specific knockdown, adhesive ability of B16BL6 melanoma cells was also significantly inhibited, which was unexpected and not reported before. These results imply that AKT3 knockdown may contribute to SBF-1's inhibition to adhesion of B16BL6 melanoma cells to fibronectin.

In vivo studies suggested that 1, 5 and 10 μg/kg SBF-1 significantly inhibited growth and weight of melanoma xenografts. 10 μg/kg SBF-1 had a comparable effect to 1 mg/kg cisplatin on tumor growth and weight, but had little effects on body weights, spleen and liver weights, implying that SBF-1 has a relatively higher therapeutic index than cisplatin. As expected, phosphorylation of AKT was significantly inhibited in a dose-dependent manner. Moreover, 1, 5 and 10 μg/kg SBF-1 greatly prolonged life span of the mice with melanoma xenografts, which were better than 1 mg/kg cisplatin did. In addition, in a mouse model of spontaneous metastasis, 1 and 3 μg/kg SBF-1 prevented B16BL6 melanoma cells in primary tumor from invading the draining lymph nodes.

In human melanoma cell line A875, we observed similar phenomenon in growth suppression. After incubation with different concentrations of SBF-1 for 72 h, growth of A875 cells were significantly inhibited (Supplementary Fig. S10A). Meanwhile, after incubation with 1000 nM SBF-1 for 24 h, cell cycle was arrested (Supplementary Fig. S10B), and phosphorylation of AKT at threonine 308 site was significantly ($P < 0.05$) reduced (Supplementary Fig. S10C). However, the influences were not so strong as growth inhibition, implying that the mechanism for SBF-1 in A875 cells was different from that in B16BL6 cells, and needs further study.

In summary, as described in Fig. 6D, our current study offers the first mechanism and the first *in vivo* evidence for SBF-1's strong antitumor effect. With this small molecular compound, we also observed previously unknown phenomenon, PDK1 only interacts with AKT3, in B16BL6 melanoma cells. Hence, a significant outcome from the current findings could be beneficial for the development of novel therapeutic agents targeting the interaction between PDK1 and AKT3 as a novel strategy for anti-melanoma therapy.

Disclosure of potential conflicts of interest

No potential conflicts of interest were disclosed.

Grant support

This work was supported by Science Fund for Creative Research Groups of NSFC (No. 81121062), National Natural Science Foundation of China (Nos. 90913023 and 81173070), National Fundamental Fund of Personnel Training in Biology (No. J1103512), National Science & Technology Major Project (No.

2012ZX09304-001), and Production-Science-Research Forward-looking Project of Jiangsu Province (BY2010138).

Appendix A. Supplementary data

Supplementary data associated with this article can be found, in the online version, at http://dx.doi.org/10.1016/j.bcp.2012.04.006.

References

[1] Linos E, Swetter SM, Cockburn MG, Colditz GA, Clarke CA. Increasing burden of melanoma in the United States. J Invest Dermatol 2009;129:1666–74.
[2] Rigel DS, Russak J, Friedman R. The evolution of melanoma diagnosis: 25 years beyond the ABCDs. CA Cancer J Clin 2010;60:301–16.
[3] Jemal A, Siegel R, Xu J, Ward E. Cancer statistics, 2010. CA Cancer J Clin 2010;60:277–300.
[4] Ugurel S. Chemotherapy in metastatic melanoma – still useful or out of date. Onkologie 2011;34:159–60.
[5] Eigentler TK, Caroli UM, Radny P, Garbe C. Palliative therapy of disseminated malignant melanoma: a systematic review of 41 randomised clinical trials. Lancet Oncol 2003;4:748–59.
[6] Sykes SM, Lane SW, Bullinger L, Kalaitzidis D, Yusuf R, Saez B, et al. AKT/FOXO signaling enforces reversible differentiation blockade in myeloid leukemias. Cell 2011;146:697–708.
[7] Li M, Li H, Li C, Wang S, Jiang W, Liu Z, et al. Alpha-fetoprotein: a new member of intracellular signal molecules in regulation of the PI3K/AKT signaling in human hepatoma cell lines. Int J Cancer 2011;128:524–32.
[8] Fenouille N, Puissant A, Tichet M, Zimniak G, Abbe P, Mallavialle A, et al. SPARC functions as an anti-stress factor by inactivating p53 through Akt-mediated MDM2 phosphorylation to promote melanoma cell survival. Oncogene 2011;30:4887–900.
[9] Vincent EE, Elder DJ, Thomas EC, Phillips L, Morgan C, Pawade J, et al. Akt phosphorylation on Thr308 but not on Ser473 correlates with Akt protein kinase activity in human non-small cell lung cancer. Br J Cancer 2011;104:1755–61.
[10] Wang Z, Li Y, Ahmad A, Banerjee S, Azmi AS, Kong D, et al. Down-regulation of Notch-1 is associated with Akt and FoxM1 in inducing cell growth inhibition and apoptosis in prostate cancer cells. J Cell Biochem 2011;112:78–88.
[11] Bos JL. A target for phosphoinositide 3-kinase: Akt/PKB. Trends Biochem Sci 1995;20:441–2.
[12] Marte BM, Downward J. PKB/Akt: connecting phosphoinositide 3-kinase to cell survival and beyond. Trends Biochem Sci 1997;22:355–8.
[13] Maroulakou IG, Oemler W, Naber SP, Tsichlis PN. Akt1 ablation inhibits, whereas Akt2 ablation accelerates, the development of mammary adenocarcinomas in mouse mammary tumor virus (MMTV)-ErbB2/neu and MMTV-polyoma middle T transgenic mice. Cancer Res 2007;67:167–77.
[14] Nitsche C, Edderkaoui M, Moore RM, Eibl G, Kasahara N, Treger J, et al. The phosphatase PHLPP1 regulates Akt2, promotes pancreatic cancer cell death, and inhibits tumor formation. Gastroenterology 2012;142. 377–387 e1–5.
[15] Shi XH, Liang ZY, Ren XY, Liu TH. Combined silencing of K-ras and Akt2 oncogenes achieves synergistic effects in inhibiting pancreatic cancer cell growth in vitro and in vivo. Cancer Gene Ther 2009;16:227–36.
[16] Ericson K, Gan C, Cheong I, Rago C, Samuels Y, Velculescu VE, et al. Genetic inactivation of AKT1, AKT2, and PDPK1 in human colorectal cancer cells clarifies their roles in tumor growth regulation. Proc Natl Acad Sci USA 2010;107:2598–603.
[17] Davies MA, Stemke-Hale K, Tellez C, Calderone TL, Deng W, Prieto VG, et al. A novel AKT3 mutation in melanoma tumours and cell lines. Br J Cancer 2008;99:1265–8.
[18] Shao Y, Aplin AE. Akt3-mediated resistance to apoptosis in B-RAF-targeted melanoma cells. Cancer Res 2010;70:6670–81.
[19] Madhunapantula SV, Robertson GP. The PTEN-AKT3 signaling cascade as a therapeutic target in melanoma. Pigment Cell Melanoma Res 2009;22:400–19.
[20] Cheung M, Sharma A, Madhunapantula SV, Robertson GP. Akt3 and mutant V600E B-Raf cooperate to promote early melanoma development. Cancer Res 2008;68:3429–39.
[21] Stahl JM, Sharma A, Cheung M, Zimmerman M, Cheng JQ, Bosenberg MW, et al. Deregulated Akt3 activity promotes development of malignant melanoma. Cancer Res 2004;64:7002–10.
[22] Ding Z, Liang J, Li J, Lu Y, Ariyaratna V, Lu Z, et al. Physical association of PDK1 with AKT1 is sufficient for pathway activation independent of membrane localization and phosphatidylinositol 3 kinase. PLoS One 2010;5:e9910.
[23] Alessi DR, James SR, Downes CP, Holmes AB, Gaffney PR, Reese CB, et al. Characterization of a 3-phosphoinositide-dependent protein kinase which phosphorylates and activates protein kinase Balpha. Curr Biol 1997;7:261–9.
[24] Gao X, Yo P, Harris TK. Improved yields for baculovirus-mediated expression of human His(6)-PDK1 and His(6)-PKBbeta/Akt2 and characterization of phospho-specific isoforms for design of inhibitors that stabilize inactive conformations. Protein Expr Purif 2005;43:44–56.
[25] Zheng D, Guan Y, Chen X, Xu Y, Lei P. Synthesis of cholestane saponins as mimics of OSW-1 and their cytotoxic activities. Bioorg Med Chem Lett 2011;21:3257–60.
[26] Maj J, Morzycki JW, Rarova L, Oklest'kova J, Strnad M, Wojtkielewicz A. Synthesis and biological activity of 22-deoxo-23-oxa analogues of saponin OSW-1. J Med Chem 2011;54:3298–305.
[27] Burgett AW, Poulsen TB, Wangkanont K, Anderson DR, Kikuchi C, Shimada K, et al. Natural products reveal cancer cell dependence on oxysterol-binding proteins. Nat Chem Biol 2011;7:639–47.
[28] Zhou Y, Garcia-Prieto C, Carney DA, Xu RH, Pelicano H, Kang Y, et al. OSW-1: a natural compound with potent anticancer activity and a novel mechanism of action. J Natl Cancer Inst 2005;97:1781–5.
[29] Shi B, Wu H, Yu B, Wu J. 23-oxa-Analogues of OSW-1: efficient synthesis and extremely potent antitumor activity. Angew Chem Int Ed Engl 2004;43:4324–7.
[30] Kubo S, Mimaki Y, Sashida Y, Nikaido T, Ohmoto T. Steroidal saponins from the rhizomes of *Smilax sieboldii*. Phytochemistry 1992;31:2445–50.
[31] Xue J, Liu P, Pan Y, Guo Z. A total synthesis of OSW-1. J Org Chem 2008;73:157–61.
[32] Yu W, Jin Z. Total synthesis of the anticancer natural product OSW-1. J Am Chem Soc 2002;124:6576–83.
[33] Song R, Qian F, Li YP, Sheng X, Cao SX, Xu Q. Phosphatase of regenerating liver-3 localizes to cyto-membrane and is required for B16F1 melanoma cell metastasis in vitro and in vivo. PLoS One 2009;4:e4450.
[34] Wang L, Gu Y, Shu Y, Shen Y, Xu Q. Integrin alpha6high cell population functions as an initiator in tumorigenesis and relapse of human liposarcoma. Mol Cancer Ther 2011;10:2276–86.
[35] Wang L, Shen Y, Song R, Sun Y, Xu J, Xu Q. An anticancer effect of curcumin mediated by down-regulating phosphatase of regenerating liver-3 expression on highly metastatic melanoma cells. Mol Pharmacol 2009;76:1238–45.
[36] Qian F, Zhang ZC, Wu XF, Li YP, Xu Q. Interaction between integrin alpha(5) and fibronectin is required for metastasis of B16F10 melanoma cells. Biochem Biophys Res Commun 2005;333:1269–75.
[37] Sun Y, Wu XX, Yin Y, Gong FY, Shen Y, Cai TT, et al. Novel immunomodulatory properties of cirsilineol through selective inhibition of IFN-gamma signaling in a murine model of inflammatory bowel disease. Biochem Pharmacol 2010;79:229–38.
[38] Perez-Tenorio G, Stal O, Group SSBC. Activation of AKT/PKB in breast cancer predicts a worse outcome among endocrine treated patients. Br J Cancer 2002;86:540–5.
[39] Vatish M, Tesfa L, Grammatopoulos D, Yamada E, Bastie CC, Pessin JE. Inhibition of Akt activity and calcium channel function coordinately drive cell-cell fusion in the BeWO choriocarcinoma placental cell line. PLoS One 2012;7:e29353.
[40] Chandarlapaty S, Sawai A, Scaltriti M, Rodrik-Outmezguine V, Grbovic-Huezo O, Serra V, et al. AKT inhibition relieves feedback suppression of receptor tyrosine kinase expression and activity. Cancer Cell 2011;19:58–71.
[41] Downward J. Mechanisms and consequences of activation of protein kinase B/Akt. Curr Opin Cell Biol 1998;10:262–7.
[42] Kushiro K, Chu RA, Verma A, Nunez NP. Adipocytes promote B16BL6 melanoma cell invasion and the epithelial-to-mesenchymal transition. Cancer Microenviron 2011. http://dx.doi.org/10.1007/s12307-011-0087-2.
[43] Zhang H, Zhu Z, McKinley JM, Meadows GG. IFN-gamma is essential for the inhibition of B16BL6 melanoma lung metastasis in chronic alcohol drinking mice. Clin Exp Metastasis 2011;28:301–7.
[44] Hotfilder M, Sondermann P, Senss A, van Valen F, Jurgens H, Vormoor J. PI3K/AKT is involved in mediating survival signals that rescue Ewing tumour cells from fibroblast growth factor 2-induced cell death. Br J Cancer 2005;92:705–10.
[45] Schmidt M, Hovelmann S, Beckers TL. A novel form of constitutively active farnesylated Akt I prevents mammary epithelial cells from anoikis and suppresses chemotherapy-induced apoptosis. Br J Cancer 2002;87:924–32.
[46] Fernandez-Herrera MA, Mohan S, Lopez-Munoz H, Hernandez-Vazquez JM, Perez-Cervantes E, Escobar-Sanchez ML, et al. Synthesis of the steroidal glycoside (25R)-3beta,16beta-diacetoxy-12,22-dioxo-5alpha-cholestan-26-yl beta-D-glucopyranoside and its anti-cancer properties on cervicouterine HeLa, CaSki, and ViBo cells. Eur J Med Chem 2010;45:4827–37.
[47] Sun L, Zhao Y, Yuan H, Li X, Cheng A, Lou H. Solamargine, a steroidal alkaloid glycoside, induces oncosis in human K562 leukemia and squamous cell carcinoma KB cells. Cancer Chemother Pharmacol 2011;67:813–21.
[48] Tejera-Vaquerizo A, Lopez-Navarro N, Alcaide-Martin A, Herrera-Acosta E, Herrera-Ceballos E. Correlation of the growth rate of melanoma with the temporal appearance of metastasis. J Eur Acad Dermatol Venereol 2011;25:366–7.
[49] Wu PR, Yen HH, Chen CJ. Gastrointestinal: primary esophageal melanoma with gastric metastasis. J Gastroenterol Hepatol 2011;26:1338.
[50] Langer HF, Orlova VV, Xie C, Kaul S, Schneider D, Lonsdorf AS, et al. A novel function of junctional adhesion molecule-C in mediating melanoma cell metastasis. Cancer Res 2011;71:4096–105.
[51] Radosavljevic G, Jovanovic I, Majstorovic I, Mitrovic M, Lisnic VJ, Arsenijevic N, et al. Deletion of galectin-3 in the host attenuates metastasis of murine melanoma by modulating tumor adhesion and NK cell activity. Clin Exp Metastasis 2011;28:451–62.